Available online at www.sciencedirect.com
ScienceDirect
Fluid Phase Equilibria 259 (2007) 89–98
FLUID PHASE EQUILIBRIA
www.elsevier.com/locate/fluid

Modeling high-pressure densities at wide temperature range with volume scaling: Cyclohexane + *n*-hexadecane mixtures

Josinira A. Amorim [a], Osvaldo Chiavone-Filho [a], Márcio L.L. Paredes [b], Krishnaswamy Rajagopal [c,*]

[a] *Departamento de Engenharia Química, PPGEQ, UFRN Campus Universitário 3000, CEP 59072-970, Brazil*
[b] *PPGEQ, Instituto de Química, UERJ, Campus Maracanã, PHLC 411, CEP 20550-900, Brazil*
[c] *DEQ, Escola de Química, UFRJ, Ilha do Fundão, CT I-122, CEP 21949-900, Brazil*

Received 31 December 2006; received in revised form 4 May 2007; accepted 10 May 2007
Available online 13 May 2007

Abstract

High-pressure density data for cyclohexane + *n*-hexadecane mixtures at a wide temperature range was modeled with several classical equations of state (EOS) and correlative models. A modification for softening the co-volume and another for a volume scaling of the Peng–Robinson EOS (VS-PR) were proposed. The VS-PR model is able to correlate the pure component experimental data employing only five adjustable parameters, with root-mean-square deviation (RMSD) between calculated and experimental densities essentially within the experimental error. This result is superior to widely used approaches, i.e., a six parameter Tait model and six parameter volume translations (temperature and pressure dependent) for Peng–Robinson and Patel–Teja EOS. The VS-PR model also represents well the isobaric thermal expansion and the isothermal compressibility coefficients of the pure cyclohexane, a small naphthenic substance as well as a long chain *n*-alkane hydrocarbon, *n*-hexadecane. When modeling the mixture data, the use of VS-PR model of pure components along with the Redlich–Kister expansion, truncated at the first term, the density was correlated within a RMSD only 60% greater than the experimental error. The proposed model is able to accurately represent all the tested mixture data with a relatively small number of parameters.

Keywords: High-pressure density; Equation of state modeling; Thermal expansion coefficient; Isothermal compressibility; Volume scaling

1. Introduction

The knowledge of the relation between thermophysical properties of mixtures and its composition is relevant in design, operation, control and optimization of industrial processes. In this sense, the knowledge of the behavior of mixture properties as a function of composition, temperature, pressure, and chemical nature of its constituents is a central question in thermodynamic modeling. Among the applications, this knowledge may be employed when using thermophysical properties as process sensors; and has been used traditionally in the characterization of complex mixtures [1], such as petroleum containing mainly non-polar substances like long chain alkane, naphthenic, and aromatic compounds, with a wide range of carbon numbers [2].

Among the thermophysical properties, density is especially important due to several formal relations between volumetric properties and other thermodynamic properties [3], besides the relations between density and other thermophysical properties. For instance, an accurate modeling of density data at different conditions allows the correct and simple computational extrapolation and interpolation of density as well as other thermodynamic functions such as specific heats.

The accurate modeling of density over a wide range of temperature and pressure is a challenging task, even for pure simple fluids. One important reason is the great impact of stiffness of the repulsive potential on density at high densities, which is not easily modeled by traditional approaches [4–6]. As an example of this difficulty, Pitzer and Sterner modeled densities of pure water and carbon dioxide over a large pressure range [4]

* Corresponding author. Tel.: +55 21 2562 7424; fax: +55 21 2562 7567.
E-mail addresses: nirinha@eq.ufrn.br (J.A. Amorim), osvaldo@eq.ufrn.br (O. Chiavone-Filho), paredes@uerj.br (M.L.L. Paredes), raja@eq.ufrj.br (K. Rajagopal).

0378-3812/$ – see front matter © 2007 Elsevier B.V. All rights reserved.
doi:10.1016/j.fluid.2007.05.007

with a multi-parameter equation. Twenty-eight parameters were needed to correlate carbon dioxide data and 27 for water which is not suitable for many engineering applications. Following Gregorowicz et al. [6], many multi-parameters equations are able to accurately represent density data, showing important experimentally observed density extrema, such as in the isothermal variation of the isochoric heat capacity, of the isothermal compressibility, speed of sound, and isobaric expansivity, which is not the case when simple models are employed [5,6]. In this work, a method is sought to improve the accuracy of simple models without enhancing significantly the number of parameters in the equation. A useful way to obtain better results from simple models based on repulsive and attractive contributions is to introduce a temperature-dependence for the co-volume [6].

Hemptinne and Ungerer [7] tested five equations of state (EOS) in the calculation of hydrocarbons high-pressure density. The EOS tested were Peng–Robinson EOS [8], volume translated Peng–Robinson, following the approach of Penéloux et al. [9], SBR EOS [10], chain-of-rotators EOS [11], Lee–Kesler model [12] and a modification of the last model. Hemptinne and Ungerer [7] pointed out as better models the modified Lee-Kesler model for small chains and chain-of-rotators EOS for higher chains. In this comparison, relative errors of 2–3% were considered moderate, and errors greater than 4% were considered high.

Sant'Ana et al. [13] compared temperature-dependent volume translation models for the prediction of hydrocarbon densities. The model of Ungerer and Batut [14] was pointed out as the most feasible choice, presenting relative deviations from 0.64 to 2.43%.

Nasrifar et al. [15] presented a corresponding states model for compressed liquid densities and compared their model with the models of Yen and Woods [16]; Chueh and Prausnitz [17]; Brelvi and O'Connell [18]; Thomson et al. [19]; Lee and Liu [20]; and Aalto et al. [21]. The authors [15] found their model superior to the other models, in the case of hydrocarbons, refrigerants and some light gases. The overall relative deviation found was 0.77%, while the deviations of the other models lied in the range 1.0–2.2%. Later, Eslami and Azin [22] presented a model for compressed liquid densities and compared their results with the models of Thomson et al. [19] and Nasrifar et al. [15], presenting accuracy similar to those obtained with the other models.

Another approach relative to high-pressure densities is the linear isotherms presented by Parsafar and Mason [23]. This observation is included in the present work as a model suitable for density calculations.

From this introduction, it can be noticed that the most accurate simple models for high-pressure liquid density reviewed here present deviations about 1% or slightly smaller, while multi-parameter equations present deviations essentially within experimental error [6]. In this sense, the actual simple models are not satisfactory for highly accurate work, and the multi-parameter models are not suitable for engineering applications which need fast implementations and calculations. This points out the importance in improving of the accuracy through simple models.

1.1. Objective

The objective of this work was to evaluate the performance of correlative simple models in order to represent high-pressure densities and its derivative with temperature and pressure as close to experimental errors as possible, and also propose a new correlative volume scaled model. Once model parameters were estimated from experimental data, the number of systems studied was restricted in order to avoid excessive and unnecessary parameter estimation.

1.2. Experimental densities and derived properties used in this work

Recently, the authors of this work obtained high pressure (up to 62.053 MPa) densities over a wide temperature range (318.15–413.15 K) for mixtures of cyclohexane and *n*-hexadecane, including pure component data. The experimental method and data are presented elsewhere [24].

This data was chosen to evaluate performances of the correlations and EOS studied in this work, because in asymmetric mixtures large differences in molecular shape, size or flexibility could cause deviations in physical properties from ideal mixture behavior, even for mixtures of non-polar substances [25]. Cyclohexane is a small naphthenic molecule while *n*-hexadecane is a long linear alkyl chain, leading to an asymmetrical mixture in length and shape of components with close densities at ambient conditions. High-pressure density for this mixture was presented previously by Tanaka et al. [26], at only three temperatures. The recent data [24] allows the study of density and derived properties of this mixture for a wider range of temperatures and compositions.

The isobaric thermal expansion (α) and the isothermal compressibility (k_T) coefficients, and excess volume (V^E) were derived from experimental [24] densities (ρ). These properties are defined, respectively, in Eq. (1)–(3):

$$\alpha(P, T, \underline{x}) = -\left[\partial\frac{\ln(\rho)}{\partial T}\right]_{P,\underline{x}} \tag{1}$$

$$k_T(P, T, \underline{x}) = \left[\partial\frac{\ln(\rho)}{\partial P}\right]_{T,\underline{x}} \tag{2}$$

$$V^E(P, T, \underline{x}) = V(P, T, \underline{x}) - (x_1 V_1(P, T) + x_2 V_2(P, T)) \tag{3}$$

where subscripts 1 and 2 stand for the pure components and V is the molar volume.

2. Methodology

Several widely used multi-parameter empirical models for pure component and mixtures selected for representing the experimental behavior of density as a function of temperature and pressure.

For pure components, a polynomial model for isobaric thermal expansion and isothermal compressibility coefficients was used. The degree of the polynomial was chosen by observing the experimental trends. For mixtures, the Redlich–Kister [27]

expansion was used. The number of terms in the expansion and the form of dependence of coefficients on temperature and pressure were chosen after examining the experimental data. As this expansion leads to root-mean-square deviations (RMSD) essentially within experimental uncertainty, both for pure component and mixtures, it was used as a benchmark for evaluating the performance of other models.

The following widely used multi-parameters models were evaluated: Tait model [28], Peng–Robinson EOS [8], Valderrama and Cisternas version of Patel–Teja EOS [29], linearity model (linear isotherms) of Parsafar and Mason [23], Peng–Robinson with volume translation and Patel–Teja EOS with volume translation as well as Peng–Robinson and Patel–Teja EOS with temperature dependent co-volume as proposed by Gregorowicz et al. [6]. The volume scaling is proposed in this work to obtain at least equal performance with fewer parameters.

For evaluating original Peng–Robinson and Patel–Teja equations, the necessary input parameters- critical temperature, critical pressure, acentric factor (Peng–Robinson) and critical compressibility factor (Patel–Teja) were obtained from [30]. In general, the evaluated models had five or six adjustable parameters, with the exception of the soft co-volume Peng–Robinson, which employs four parameters. The widely used models with six parameters presented a performance worse than the proposal of this work (volume scaled Peng–Robinson, which employs five parameters).

Besides RMSD (Eq. (4)), the average absolute relative deviation (AAD, Eq. (5)) was also calculated in order to compare with literature results:

$$\mathrm{RMSD} = \sqrt{\sum_{i=1}^{N} \frac{(\rho_i^{\mathrm{calc}} - \rho_i^{\mathrm{exp}})^2}{N}} \tag{4}$$

$$\mathrm{AAD} = \sum_{i=1}^{N} \frac{|(\rho_i^{\mathrm{calc}} - \rho_i^{\mathrm{exp}})/\rho_i^{\mathrm{exp}}|}{N} \tag{5}$$

where N is the number of points, i runs over experimental points superscripts calc and exp stand for calculated and experimental, respectively.

The parameter estimations procedure minimized RMSD using the Simplex [31] numerical method. In order to avoid local minimum solutions, the initial guesses for pure component models parameters were obtained by applying the model in the correlation of density as a function of pressure for each temperature, and then the temperature dependence for the optimized parameters was introduced and the parameters re-estimated. For mixtures, the number of parameters was small in general, and multiple initial guesses were tried.

3. Correlation of pure component high-pressure densities

In this section, the pure component models evaluated in this work are presented.

3.1. Empirical polynomial model from α and k_T (polynomial)

The density model is obtained after integration of Eq. (1) at a given pressure P^*, from a given temperature T^* to a temperature T. A density value at T^* and P^* must be known, and here values presented by Amorim et al. [24] were used. The final step is to integrate Eq. (2) from P^* to a pressure P. The model equations and the 12 adjustable parameters (a's, b's and c's indices 0–2) are presented as follows:

$$\alpha(T, P^*) = a' + b'T + c'T^2 \tag{6}$$

$$k_{\mathrm{T}}(T, P) = a(P) + b(P)T + c(P)T^2 \tag{7}$$

$$\begin{aligned} a(P) &= a_0^{\mathrm{P}} + a_1^{\mathrm{P}}P + a_2^{\mathrm{P}}P^2, \\ b(P) &= b_0^{\mathrm{P}} + b_1^{\mathrm{P}}P + b_2^{\mathrm{P}}P^2, \\ c(P) &= c_0^{\mathrm{P}} + c_1^{\mathrm{P}}P + c_2^{\mathrm{P}}P^2 \end{aligned} \tag{8}$$

3.2. Tait empirical model (Tait)

The Tait [28] model (Eq. (9)) was used with all adjustable parameters as temperature dependent. This dependency (Eq. (10)) was chosen after the initial guess procedure presented in Section 2. The model has six (ρ_0^0, ρ_1^0, B_0, B_1, C_0, C_1) adjustable parameters:

$$\rho(T, P) = \frac{\rho^0(T)}{\{1 + C(T)\ln[(B(T) + 0.1)/(B(T) + P)]\}} \tag{9}$$

$$\begin{aligned} &\rho_0(T) = \rho_0^0 + \rho_1^0 T, \qquad C(T) = C_0 + C_1 T, \\ &B(T) = B_0 + B_1 T \end{aligned} \tag{10}$$

3.3. Empirical linearity between $(Z-1)V$ and ρ_m^2 (linearity)

The Parsafar and Mason [23] isothermal linearity involving compressibility factor Z and the molar density ρ_{m} may be obtained from the virial expansion truncated at the fourth coefficient, but neglecting the third one. In this work, the third coefficient is also included, but not as a temperature function (Eq. (11)), in order to enhance model performance and equalize the number of parameters. The temperature dependences in Eq. (12) followed procedure presented in Section 2. The model has five adjustable parameters, a_0^{L}, a_1^{L}, b_0^{L}, b_1^{L} and c^{L}:

$$(Z-1)V = a(T) + b(T)\rho_{\mathrm{m}}^2 + c^{\mathrm{L}}\rho_{\mathrm{m}} \tag{11}$$

$$a(T) = a_0^{\mathrm{L}} + \frac{a_1^{\mathrm{L}}}{T}, \qquad b(T) = b_0^{\mathrm{L}} + \frac{b_1^{\mathrm{L}}}{T} \tag{12}$$

3.4. Peng–Robinson EOS (PR)

The equations for the original Peng–Robinson EOS are presented as follows:

$$P = \frac{RT}{V-b} - \frac{a_c[1+k(1-\sqrt{T/T_c})]^2}{V^2+2bV-b^2} \tag{13}$$

$$a_c = \frac{0.4572355\,(RT_c)^2}{P_c}, \qquad b = \frac{0.07779607RT_c}{P_c} \tag{14}$$

3.5. Patel–Teja EOS (PT)

The Valderrama and Cisternas version of the Patel–Teja EOS is given in Eq. (15) and (16):

$$P = \frac{RT}{V-b} - \frac{a_c[1+k(1-\sqrt{T/T_c})]^2}{V^2+(b+c)V-bc} \tag{15}$$

$$a_c = \Omega_a(Z_c)\frac{(\mathrm{RT_c})^2}{P_c}, \qquad b = \Omega_b(Z_c)\frac{RT_c}{P_c},$$
$$c = \Omega_c(Z_c)\frac{RT_c}{P_c} \tag{16}$$

3.6. Volume translated Peng–Robinson EOS (PR-t)

The volume translation method [9,13] was applied to Peng–Robinson EOS (superscript PR stands for original EOS) with the translated volume (indicated by superscript t, Eq. (17)) a function of pressure and temperature, with these functions obtained in the procedure described in Section 2, and given in Eqs. (18) and (19). The model has six adjustable pure component parameters (v_{00}^{PR}, v_{01}^{PR}, v_{10}^{PR}, v_{11}^{PR}, v_{20}^{PR}, v_{21}^{PR}).

$$V(T,P) = V^{PR}(T,P) - V^{t}(T,P) \tag{17}$$

$$V^{t}(T,P) = V_0(T) + V_1(T)P + V_2(T)P^2 \tag{18}$$

$$V_0(T) = v_{00}^{PR} + v_{01}^{PR}T, \qquad V_1(T) = v_{10}^{PR} + v_{11}^{PR}T,$$
$$V_2(T) = v_{20}^{PR} + v_{21}^{PR}T \tag{19}$$

3.7. Volume translated Patel–Teja EOS (PT-t)

Follows procedure analogous to the previous model. The model equations are

$$V(T,P) = V^{PT}(T,P) - V^{t}(T,P) \tag{20}$$

$$V^{t}(T,P) = V_0(T) + V_1(T)P + V_2(T)P^2 \tag{21}$$

$$V_0(T) = v_{00}^{PT} + v_{01}^{PT}T, \qquad V_1(T) = v_{10}^{PT} + v_{11}^{PT}T,$$
$$V_2(T) = v_{20}^{PT} + v_{21}^{PT}T \tag{22}$$

3.8. Peng–Robinson EOS with soft co-volume (PR-b)

In this approach, the co-volume is a function of temperature in the same way as parameter a, and the critical temperature and pressure are replaced by the adjustable parameters τ^{PR} and π^{PR}. Also, the constant k is no longer related to acentric factor, but is another adjustable parameter along with λ^{PR}. The model equations are

$$P = \frac{RT}{V-b(T)} - \frac{a_c[1+k^{PR}(1-\sqrt{T/\tau^{PR}})]^2}{V^2+2b(T)V-b(T)^2} \tag{23}$$

$$b(T) = b_c[1+\lambda^{PR}(1-\sqrt{T/\tau^{PR}})]^2 \tag{24}$$

$$a_c = \frac{0.4572355(R\tau^{PR})^2}{\pi^{PR}}, \qquad b_c = \frac{0.07779607R\tau^{PR}}{\pi^{PR}} \tag{25}$$

3.9. Patel–Teja EOS with soft co-volume (PT-b)

Follows the same procedure of the previous model, and the five adjustable parameters are τ^{PT}, π^{PT}, k^{PT}, λ^{PT} and ζ^{PT}:

$$P = \frac{RT}{V-b(T)} - a_c\frac{[1+k^{PT}(1-\sqrt{T/\tau^{PT}})]^2}{V^2+(b(T)+c)V-b(T)c} \tag{26}$$

$$b(T) = b_c[1+\lambda^{PT}(1-\sqrt{T/\tau^{PT}})]^2 \tag{27}$$

$$a_c = \Omega_a(\zeta^{PT})\frac{(R\tau^{PT})^2}{\pi^{PT}}, \qquad b_c = \Omega_b(\zeta^{PT})\frac{R\tau^{PT}}{\pi^{PT}},$$
$$c = \Omega_c(\zeta^{PT})\frac{R\tau^{PT}}{\pi^{PT}} \tag{28}$$

3.10. Scaled volume Peng–Robinson EOS (VS-PR)

Again the PR EOS was used in order to correlate the experimental data, the original equations presented in Eqs. (13) and (14) being now replaced by Eqs. (29) and (30) where, analogously to the procedure presented for the PR-b, the critical constants are changed by adjustable parameters:

$$P = \frac{RT}{V-b} - a_c\frac{[1+k^{VS-PR}(1-\sqrt{T/\tau^{VS-PR}})]^2}{V^2+2bV-b^2} \tag{29}$$

$$a_c = 0.4572355\frac{(R\tau^{VS\text{-}PR})^2}{\pi^{VS\text{-}PR}}, \qquad b_c = 0.07779607\frac{R\tau^{VS\text{-}PR}}{\pi^{VS\text{-}PR}} \tag{30}$$

Since this model could not accurately correlate the isobaric thermal expansion in all ranges of pressure and simultaneously correlate accurately the density data, the strategy adopted was to obtain the model parameters ($\tau^{VS\text{-}PR}$, $\pi^{VS\text{-}PR}$ and $k^{VS\text{-}PR}$) so that k_T was accurately correlated. It was found that the experimental and the calculated density were directly proportional. For this reason, a volume scaling function $a^s(T)$ was applied, as

presented in Eq. (31), where M is the molecular weight:

$$\rho^{\text{calc}} = \rho^{\text{EOS}} \frac{a^{\text{s}}(T)}{M} \tag{31}$$

$$a^{\text{s}}(T) = a_0^{\text{s}} + \frac{a_1^{\text{s}}}{T} \tag{32}$$

The proposal uses five adjustable parameters: $\tau^{\text{VS-PR}}$, $\pi^{\text{VS-PR}}$, $k^{\text{VS-PR}}k$, a_0^{s} and a_1^{s}.

4. Correlation of mixture high-pressure densities

This section presents the mixture models based on the Redlich–Kister expansion and on the VS-PR model.

4.1. Empirical Redlich–Kister polynomial model for V^E (Redlich–Kister)

The Redlich–Kister expansion truncated at the second term was used in order to correlate the experimental data of binary mixtures, using a simple linear dependence with pressure, and quadratic and linear dependences with temperature, as presented in Eqs. (33)–(36). This approach employed experimental pure component data and ten adjustable parameters (a's and b's indices 00, 01, 02, 10 and 11):

$$V^{\text{E}}(P, T, \underline{x}) = x_1 x_2 [A(P, T) + B(P, T)(x_1 - x_2)] \tag{33}$$

$$A(P, T) = A_0(T) + A_1(T)P, \quad B(P, T) = B_0(T) + B_1(T)P \tag{34}$$

$$A_0(T) = a_{00} + a_{01}T + a_{02}T^2, \quad A_1(T) = a_{10} + a_{11}T \tag{35}$$

$$B_0(T) = b_{00} + b_{01}T + b_{02}T^2, \quad B_1(T) = b_{10} + b_{11}T \tag{36}$$

4.2. Redlich–Kister truncated at the first term (Redlich–Kister 2)

A simplified version of the previous model was used by truncating the Redlich–Kister expansion after the first term, which was considered constant (one adjustable parameter for a binary mixture):

$$V^{\text{E}}(P, T, \underline{x}) = x_1 x_2 A \tag{37}$$

4.3. VS-PR with mixing and combining rules (VS-PR mix)

The mixing rules used were

$$a(T) = \sum_i \sum_j x_i x_j a_{ij}(T), \qquad b = \sum_i \sum_j x_i x_j b_{ij},$$

$$a^{\text{s}}(T) = \sum_i \sum_j x_i x_j a_{ij}^{\text{s}}(T) \tag{38}$$

where i and j runs over all components, and the combining rules were

$$a_{ij}(T) = \sqrt{a_i(T) a_j(T)}(1 - k_{ij}) \tag{39}$$

$$b_{ij} = \frac{(1 - l_{ij})(b_i + b_j)}{2} \tag{40}$$

$$a_{ij}^{\text{s}}(T) = (1 - m_{ij}) \frac{a_i^{\text{s}}(T) + a_j^{\text{s}}(T)}{2} \tag{41}$$

The three adjustable parameters are k_{ij}, l_{ij} and m_{ij}. As usual in this approach, $k_{ii} = l_{ii} = m_{ii} = 0$ and $k_{ij} = k_{ji}$; $l_{ij} = l_{ji}$ and $m_{ij} = m_{ji}$.

4.4. VS-PR mix re-estimating pure component parameters (VS-PR mix 2)

The previous approach was used also re-estimating the pure components parameters, leading to thirteen parameters for a binary mixture (five for each pure component, plus the three k_{12}, l_{12} and m_{12}).

4.5. VS-PR with Redlich–Kister 2 (VS-PR mix 3)

A hybrid model was set up by using VS-PR for the pure component calculation and Eq. (37) for a binary mixture calculation, employing one adjustable parameter (A).

5. Results and discussion

This section presents the results separately for the pure and the mixture models.

5.1. Pure component models

The RMSD between calculated and experimental [24] pure components cyclohexane and n-hexadecane densities are presented in Table 1, obtained after estimation of the model parameters. The regressed parameters are presented in Table 2.

As it can be observed, the *Tait* model presents deviations of 1.5 and 2.0 times the reference deviation of *Polynomial* correlation (for cyclohexane and n-hexadecane, respectively), while linear isotherms model presents the values of 2.0 and 1.5. These performances are considered as in good agreement with experimental data. The larger deviations occur for the

Table 1
RMSD between calculated and experimental pure component densities

Model	Parameters[a]	RMSD (kg m^{-3})	
		Cyclohexane	n-Hexadecane
Polinomial	12	0.28	0.23
Tait	6	0.42	0.47
Linearity	5	0.56	0.34
PR	0	49.27	122.79
PT	0	28.10	84.33
PR-t	6	0.60	0.67
PT-t	6	0.64	0.70
PR-b	4	0.76	1.46
PT-b	5	0.31	0.85
PR-VS	5	0.30	0.27

[a] Number of parameters estimated using the pure component data reported in Ref. [24].

Table 2
Parameters obtained with the models

Parameter	Cyclohexane	*n*-Hexadecane
Polynomial		
a' (K^{-1})	1.2454×10^{-3}	8.2081×10^{-4}
b' (K^{-2})	-2.3272×10^{-5}	-1.0113×10^{-5}
c' (K^{-3})	2.1258×10^{-7}	4.6730×10^{-8}
a_0^P (MPa^{-1})	2.8380×10^{-3}	6.8319×10^{-3}
a_1^P ($MPa^{-1}\,K^{-1}$)	-5.8596×10^{-6}	4.8000×10^{-5}
a_2^P ($MPa^{-1}\,K^{-2}$)	-1.0112×10^{-6}	-3.1334×10^{-6}
b_0^P ($MPa^{-1}\,K^{-1}$)	-1.1700×10^{-5}	-3.5225×10^{-5}
b_1^P ($MPa^{-1}\,K^{-2}$)	7.7127×10^{-8}	-2.9664×10^{-7}
b_2^P ($MPa^{-1}\,K^{-3}$)	4.9754×10^{-9}	1.7618×10^{-8}
c_0^P ($MPa^{-1}\,K^{-2}$)	2.1438×10^{-8}	5.2277×10^{-8}
c_1^P ($MPa^{-1}\,K^{-3}$)	-2.7779×10^{-10}	3.9049×10^{-10}
c_2^P ($MPa^{-1}\,K^{-4}$)	-5.2887×10^{-12}	-2.4281×10^{-11}
Tait		
ρ_0^0 ($kg\,m^{-3}$)	1.0737×10^{3}	9.7118×10^{2}
ρ_1^0 ($kg\,m^{-3}\,K^{-1}$)	-1.0052	-6.8027×10^{-1}
B_0 (MPa^{-1})	6.0819×10^{1}	-1.3895×10^{1}
B_1 ($MPa^{-1}\,K^{-1}$)	-6.6629×10^{-2}	1.8296×10^{-1}
C_0	-7.1563×10^{-2}	-1.2327×10^{-1}
C_1 (K^{-1})	4.2074×10^{-4}	5.5227×10^{-4}
Linearity		
a_0^L ($m^3\,mol^{-1}$)	5.9212×10^{-3}	5.6852×10^{-2}
a_1^L ($m^3\,mol^{-1}\,K$)	-4.5925×10^{-1}	-7.3981
b_0^L ($m^9\,mol^{-3}$)	1.0005×10^{-10}	4.9756×10^{-9}
b_1^L/($m^9\,mol^{-3}\,K^{-1}$)	4.0618×10^{-10}	4.0780×10^{-7}
c^L ($m^6\,mol^{-2}$)	-1.6871×10^{-5}	-1.3704×10^{-4}
PR-t		
v_{00}^{PR} ($m^3\,mol^{-1}$)	-2.7304×10^{-6}	9.5454×10^{-5}
v_{01}^{PR} ($m^3\,mol^{-1}\,K^{-1}$)	-1.0224×10^{-8}	-1.0706×10^{-7}
v_{10}^{PR} ($m^3\,mol^{-1}\,MPa^{-1}$)	2.3892×10^{-7}	1.8087×10^{-7}
v_{11}^{PR} ($m^3\,mol^{-1}\,K^{-1}\,MPa^{-1}$)	-7.6150×10^{-10}	-4.9392×10^{-10}
v_{20}^{PR} ($m^3\,mol^{-1}\,MPa^{-2}$)	-2.1654×10^{-9}	-1.8950×10^{-9}
v_{21}^{PR} ($m^3\,mol^{-1}\,K^{-1}\,MPa^{-2}$)	7.3042×10^{-12}	7.1697×10^{-12}
PT-t		
v_{00}^{PT} ($m^3\,mol^{-1}$)	-1.3013×10^{-6}	7.7589×10^{-5}
v_{01}^{PT} ($m^3\,mol^{-1}\,K^{-1}$)	-6.5016×10^{-9}	-1.1560×10^{-7}
v_{10}^{PT} ($m^3\,mol^{-1}\,MPa^{-1}$)	2.5142×10^{-7}	1.4476×10^{-7}
v_{11}^{PT} ($m^3\,mol^{-1}\,K^{-1}\,MPa^{-1}$)	-8.0460×10^{-10}	-3.7086×10^{-10}
v_{20}^{PT} ($m^3\,mol^{-1}\,MPa^{-2}$)	-2.2293×10^{-9}	-1.6801×10^{-9}
v_{21}^{PT} ($m^3\,mol^{-1}\,K^{-1}\,MPa^{-2}$)	7.5078×10^{-12}	6.4818×10^{-12}
PR-b		
τ^{PR} (K)	6.3531×10^{2}	7.6480×10^{2}
π^{PR} (MPa)	3.9696	1.5824
k^{PR}	1.5485×10^{-1}	3.9321×10^{-1}
λ^{PR}	-1.7473×10^{-1}	-2.0268×10^{-1}
PT-b		
τ^{PT} (K)	6.4095×10^{2}	1.1514×10^{3}
π^{PT} (MPa)	7.0140	1.1026×10^{1}
k^{PT}	1.1690	1.8974×10^{1}
λ^{PT}	-1.0914×10^{-1}	-1.8168×10^{-1}
ζ^{PT}	4.8778×10^{-1}	1.3086
VS-PR		
$\tau^{VS\text{-}PR}$ (K)	6.3258×10^{2}	7.4904×10^{2}
$\pi^{VS\text{-}PR}$ (MPa)	1.1997×10^{1}	3.3736×10^{1}
$k^{VS\text{-}PR}$	-8.6059×10^{-2}	-4.4141×10^{-1}
a_0^s ($kg\,mol^{-1}$)	3.1805×10^{-2}	1.5871×10^{-2}
a_1^s ($kg\,mol^{-1}\,K^{-1}$)	4.5999×10^{-1}	-3.5436×10^{-1}

Table 2 (*Continued*)

Parameter	Cyclohexane	*n*-Hexadecane
VS-PR mix 2		
$\tau^{VS\text{-}PR}$ (K)	6.2890×10^{2}	7.5830×10^{2}
$\pi^{VS\text{-}PR}$ (MPa)	1.9956×10^{1}	4.1785×10^{1}
$k^{VS\text{-}PR}$	-2.4980×10^{-1}	-5.0870×10^{-1}
a_0^s ($kg\,mol^{-1}$)	2.1365×10^{-2}	1.3451×10^{-2}
a_1^s ($kg\,mol^{-1}\,K^{-1}$)	-1.830×10^{-1}	-3.420×10^{-1}

PR EOS, followed by the PT EOS, which are respectively in the order of 176 and 100 times the reference for cyclohexane, and 534 and 367 times for *n*-hexadecane, which are very poor results.

The volume translations for PR and PT EOS lead to great improvement, with similar results for both substances, presenting deviations 2.1 and 2.3 times the reference for cyclohexane and 2.9 and 3.0 times for *n*-hexadecane. The soft volume correction in the PR-b, with four parameters instead of six in the volume translation, presented poorer performance, with deviations 2.7 and 6.3 times the reference, while for PT-b, with five parameters, the results were 1.1 and 3.7 times the reference value, respectively, for cyclohexane and *n*-hexadecane.

The RMSD closest to the benchmark equation was obtained by the VS-PR model, with deviations essentially within experimental error, 1.1 and 1.2 times the reference error. Neither *Tait* model nor volume translation was able to achieve the same performance, even with one more parameter. For comparison with literature results, the AAD obtained with VS-PR model was 0.03% for both pure substances, what is far below the 1% usually reported. The minimum and maximum relative deviations, are −0.08 and +0.06% for cyclohexane and −0.06 and +0.10% for *n*-hexadecane. This result presents a useful way to accurately correlate compressed liquid densities of pure fluids with a small number of parameters.

Figs. 1–6 show comparison between calculated and experimental values of density, isothermal compressibility and isobaric thermal expansion coefficient for pure fluids. In order to perform a comparison between VS-PR and a classical correlative model, *Tait* equation was chosen due to the small RMSD obtained with this model for the two pure fluids studied.

In Figs. 1 and 2, a very good agreement can be found between the calculated and experimental data for both models while correlating densities of the two fluids.

Although densities are well correlated for both models, the analysis of derivative properties show greater differences in the quality of correlations. The isobaric thermal expansion coefficient presented in Figs. 5 and 6 is better described by VS-PR than by *Tait* model. A second derivative property for density, the derivative of k_T with pressure, is also better represented by VS-PR. For both substances, at the highest temperature *Tait* model lead to underestimation of k_T at low pressures and overestimation at high pressures, while at the lowest temperature the opposite occurs. This effect was not found for VS-PR, which represented very well this property.

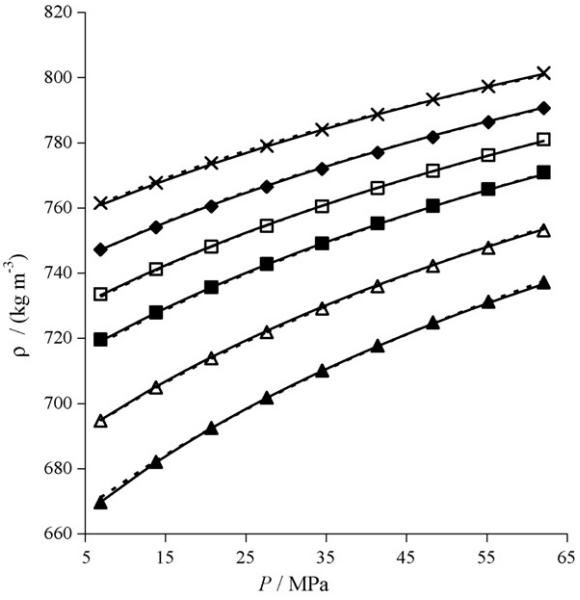

Fig. 1. Experimental (symbols) and calculated densities for cyclohexane as a function of pressure at several temperatures. Solid lines for VS-PR and dot lines for *Tait*. ×318.15 K; (♦) 333.15 K; (□) 348.15 K; (■) 363.15 K; (△) 388.15 K; (▲) 413.15 K.

For isobaric thermal expansion coefficient, again VS-PR model presented better performance than *Tait* model, with a very good agreement between experimental and correlated data for cyclohexane, and a good agreement for *n*-hexadecane. A remarkable point is that both models were not able to represent the second derivative of α with temperature (a third derivative for density) at some pressures.

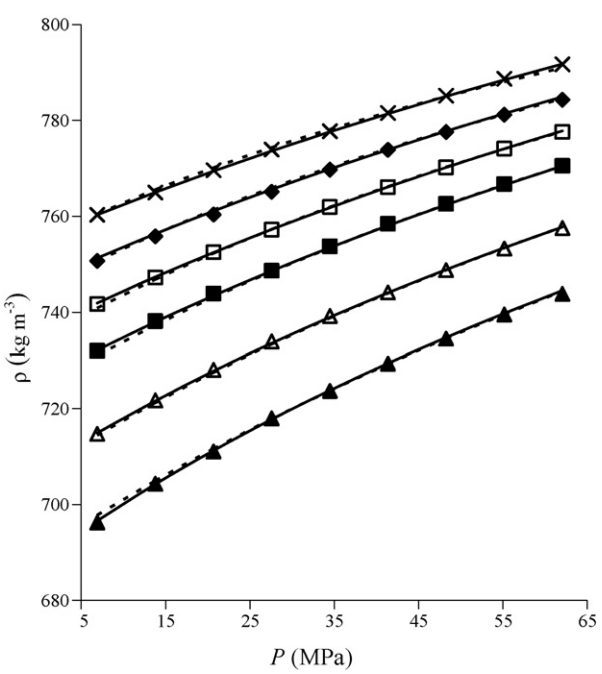

Fig. 2. Experimental (symbols) and calculated densities for *n*-hexadecane as a function of pressure at several temperatures. Solid lines for VS-PR and dot lines for *Tait*. ×318.15 K; (♦) 333.15 K; (□) 348.15 K; (■) 363.15 K; (△) 388.15 K; (▲) 413.15 K.

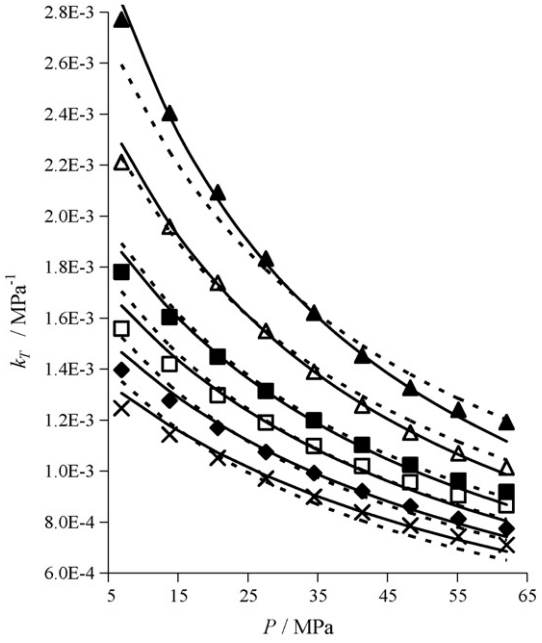

Fig. 3. Experimental (symbols) and calculated isothermal compressibility coefficients for cyclohexane as a function of pressure at several temperatures. Solid lines for VS-PR and dot lines for *Tait*. ×318.15 K; (♦) 333.15 K; (□) 348.15 K; (■) 363.15 K; (△) 388.15 K; (▲) 413.15 K.

5.2. Mixture models

The RMSD between calculated and experimental densities are presented in Table 3. The regressed mixture parameters are

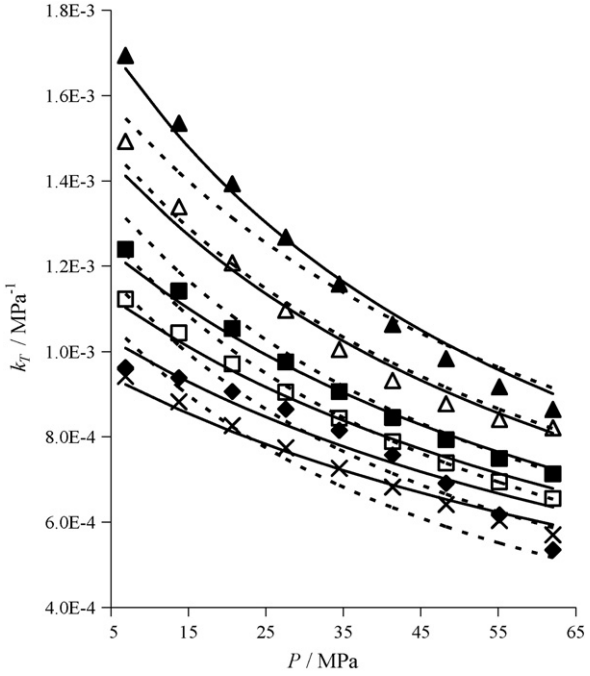

Fig. 4. Experimental (symbols) and calculated isothermal compressibility coefficients for *n*-hexadecane as a function of pressure at several temperatures. Solid lines for VS-PR and dot lines for *Tait*. ×318.15 K; (♦) 333.15 K; (□) 348.15 K; (■) 363.15 K; (△) 388.15 K; (▲) 413.15 K.

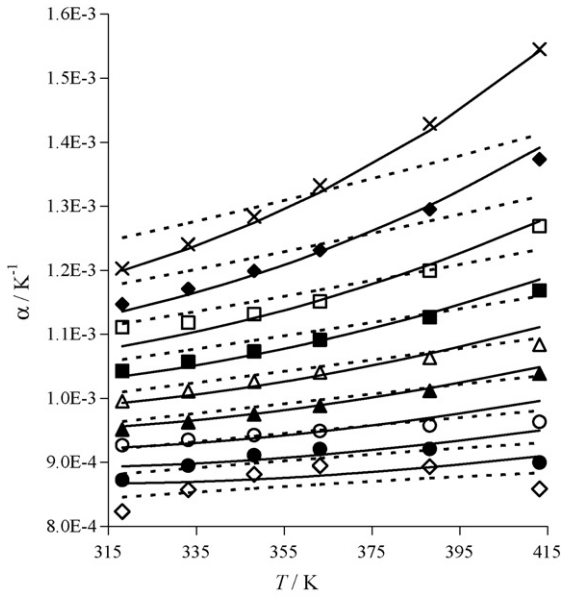

Fig. 5. Experimental (symbols) and calculated isobaric thermal expansion coefficients for cyclohexane as a function of temperature at several pressures (legend is for pressures in MPa). Solid lines for VS-PR and dot lines for *Tait*. ×6.895 MPa; (♦) 13.790 MPa; (□) 20.684 MPa; (■) 27.579 MPa; (△) 34.474 MPa; (▲) 41.369 MPa; (◯) 48.263 MPa; (●) 55.158 MPa; (◊) 62.053 MPa.

presented in Table 4 and the pure components parameters are presented in Table 2.

The density deviation of the reference model (Redlich–Kister) is higher than the deviations of the pure fluids reference model, but still is essentially within experimental error [24]. It can be noticed that using only one parameter (Redlich–Kister 2) leads to a deviation of only 1.5 times the reference deviation, obtained with a 10 parameter model. In fact, the ideal solution consideration (Redlich–Kister 2 with $A = 0$) leads to a deviation of only 3.3 times the reference, which is an indication of near ideality in this property.

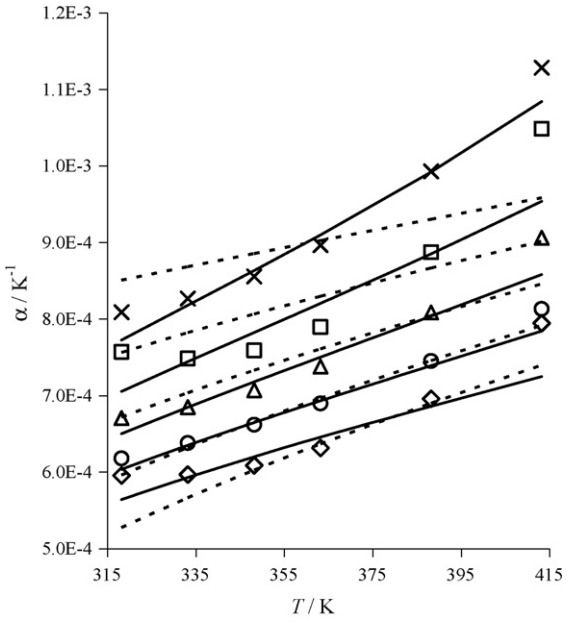

Fig. 6. Experimental (symbols) and calculated isobaric thermal expansion coefficients for *n*-hexadecane as a function of temperature at several pressures (legend is for pressures in MPa). Solid lines for VS-PR and dot lines for *Tait*. × 6.895 MPa; (□) 20.684 MPa; (△) 34.474 MPa; (◯) 48.263 MPa; (◊) 62.053 MPa.

Table 3
RMSD between calculated and experimental densities

Model	Parameters[a]	RMSD (kg m^{-3})
Redlich–Kister	10[b]	0.43
Redlich–Kister 2	1[b]	0.64
	$A = 0$[b]	1.42
VS-PR mix	3	0.98
	$k_{12} = l_{12} = m_{12} = 0$	11.52
VS-PR mix 2	13	0.69
VS-PR mix 3	1	0.69

[a] Number of parameters estimated using the data reported in Ref. [24].
[b] Experimental pure component data is informed in this approach and not counted in the number of parameters of the model.

However, the use of VS-PR mix with the three parameters set equal to zero leads to a deviation about 27 times the reference. Estimating the three parameters, for all compositions, decrease the deviation to 2.3 times the reference. Indeed, for these nearly ideal mixtures, the best VS-PR result was VS-PR mix 3, with only one mixture parameter and deviation 1.6 times the reference value. The same RMSD was obtained with VS-PR mix 2, which had thirteen parameters estimated (although 10 parameters are for the pure components).

In spite of this result being a little poorer than that of the pure components, the use of only one Redlich–Kister parameter,

Table 4
Parameters obtained with the model for mixture

Parameter	Value
Redlich–Kister	
a_{00} (m^3 mol^{-1})	3.9395×10^{-5}
a_{01} (m^3 mol^{-1} K^{-1})	-1.9104×10^{-7}
a_{02} (m^3 mol^{-1} K^{-2})	2.3668×10^{-10}
a_{10} (m^3 mol^{-1} MPa^{-1})	-9.7552×10^{-8}
a_{11} (m^3 mol^{-1} K^{-1} MPa^{-1})	2.9336×10^{-10}
b_{00} (m^3 mol^{-1})	9.8637×10^{-5}
b_{01} (m^3 mol^{-1} K^{-1})	-5.1222×10^{-7}
b_{02} (m^3 mol^{-1} K^{-2})	6.6162×10^{-10}
b_{10} (m^3 mol^{-1} MPa^{-1})	-7.5515×10^{-8}
b_{11} (m^3 mol^{-1} K^{-1} MPa^{-1})	2.1621×10^{-10}
Redlich–Kister 2	
A (m^3 mol^{-1})	2.0472×10^{-6}
VS-PR mix 3	
A (m^3 mol^{-1})	2.0782×10^{-6}
VS-PR mix	
k_{ij}	−0.7710
l_{ij}	−0.4439
m_{ij}	−0.3815
VS-PR mix 2	
k_{ij}	−0.3270
l_{ij}	−0.1860
m_{ij}	−0.1420

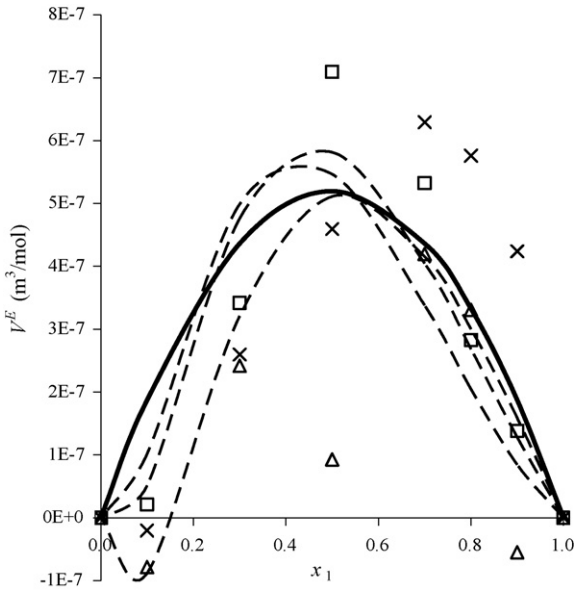

Fig. 7. Experimental (symbols) and calculated excess volumes for cyclohexane/*n*-hexadecane mixtures as a function of cyclohexane composition at 34.474 MPa and at several temperatures. Dashed lines for *VS-PR mix 2* and solid line for VS-PR mix 3. ×318.15 K; (□) 348.15 K; (△) 388.15 K.

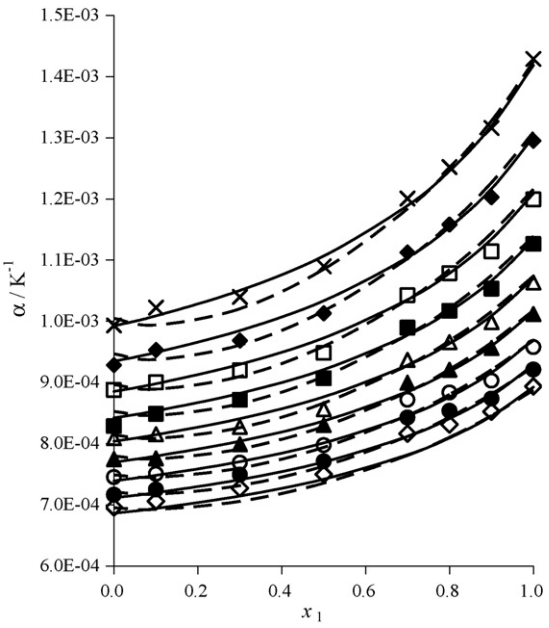

Fig. 9. Experimental (symbols) and VS-PR mix 2 calculated isobaric thermal expansion coefficients for cyclohexane/*n*-hexadecane mixtures as a function of cyclohexane composition at 388.15 K and at several pressures. Dashed lines for VS-PR mix 2 and solid lines for VS-PR mix 3. ×6.895 MPa; (♦) 13.790 MPa; (□) 20.684 MPa; (■) 27.579 MPa; (△) 34.474 MPa; (▲) 41.369 MPa; (◯) 48.263 MPa; (●) 55.158 MPa; (◊) 62.053 MPa.

leading to symmetry in the excess volume correlation, seems to be compatible with the experimental error.

Figs. 7–9 show comparisons between experimental mixture data and the VS-PR mix 2 and VS-PR mix 3 calculations for excess volume, isothermal compressibility and isobaric thermal expansion coefficient as functions of composition. The two former properties are presented at a fixed pressure (a middle value was chosen) and the last at a fixed temperature (also, a middle value was chosen).

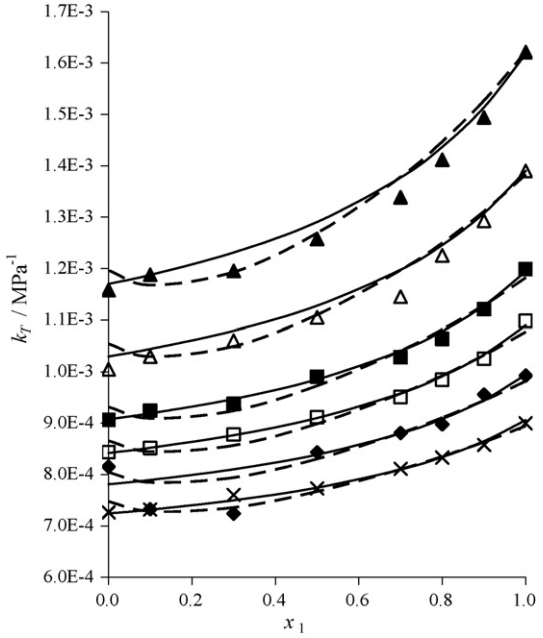

Fig. 8. Experimental (symbols) and calculated isothermal compressibility coefficients for cyclohexane/*n*-hexadecane mixtures as a function of cyclohexane composition at 34.474 MPa and at several temperatures. Dashed lines for VS-PR mix 2 and solid lines for VS-PR mix 3. ×318.15 K; (♦) 333.15 K; (□) 348.15 K; (■) 363.15 K; (△) 388.15 K; (▲) 413.15 K.

Once the excess volume calculated with the VS-PR mix 3 model is independent of temperature and pressure, only one curve is presented for all temperatures observed. Due to the low values of V^E, the experimental uncertainty leads to a great relative error for this property. As it can be seen, both VS-PR mix 2 and VS-PR mix 3 were able to represent the magnitude of the property. At low cyclohexane concentrations, VS-PR mix 2 presented V^E decreasing with increasing temperature, what could not be confirmed from the experimental data in Fig. 7.

Fig. 8 shows k_T data as a function of composition at 34.474 MPa. A significant difference between VS-PR mix 2 and VS-PR mix 3 performances is that the former presents a great concavity in this function than the last model does at about mole fraction 0.3 in cyclohexane, what is experimentally confirmed only at the two highest temperatures. It is important to notice that VS-PR mix 3 leads to ideal solution calculations for k_T and α mixture properties.

Analogously, VS-PR mix 2 presents a greater concavity than VS-PR mix 3 in Fig. 9, at about mole fraction 0.3 in cyclohexane, which is experimentally confirmed at middle pressures (13.790–41.369 MPa) only.

6. Conclusion

The densities of binary mixtures of cyclohexane and *n*-hexadecane (including pure components) were modeled in the temperature range of 388.15–413.15 K and pressures up to 62.053 MPa through classical EOS and correlation models,

along with the proposals of this work for a soft co-volume for the Peng–Robinson and Patel–Teja EOS, and a volume scaled Peng–Robinson model (VS-PR). The VS-PR model correlates pure component experimental densities with deviations essentially within experimental error, needing only five adjustable parameters. The performance of the proposed model was superior to those of classical approaches, e.g. Tait and volume translation models. Moreover, the isobaric thermal expansion and the isothermal compressibility coefficients were also very well described by the model.

When modeling the mixture data, due to the near ideality of the mixture, the best choice seems to be calculating pure component densities with the VS-PR model and estimating the first term constant parameter of the Redlich–Kister expansion, which leads to a deviation 1.6 times the estimated experimental error. An alternative with the same deviation was to include mixing and combining rules and three binary adjustable parameters, and re-estimate the pure component parameters. The two alternatives led to a good representation of mixture properties, with one superior to the other at some conditions. This switch in best model performance indicates that the hypothesis of ideality is not suitable for all conditions studied, if high accuracy is needed.

Although only one mixture was studied, the presence of short and long chain hydrocarbons, with mixture asymmetry in chain length, allowed an interesting test for the proposed modeling.

These results point out to a promising tool in correlating accurately experimental densities of pure compressed fluids, with only a few parameters (five), with better results than classical approaches. For near ideal mixtures, one more parameter is necessary for accurate modeling. Furthermore, efforts are needed if accuracy is desired in higher order derivatives of density with respect to temperature, pressure, and composition, which can be easily done in this framework by, for example, by proposing other temperature dependencies for the volume scaling function.

Acknowledgments

The authors acknowledge ANP/MCT for the scholarship to Josinira A. Amorim, the financial support of Projeto MCT/FINEP-01.06.1036-00-Temas Estratégicos 01/2006 “Distribuição do Gás Sulfídrico entre Óleos Pesados, Gás Liberado e a Água de Formação nas Condições de Reservatório”, and of PROCAD/CAPES as well as CNPq for the scholarship“bolsa de produtividade” awarded to K. Rajagopal and O. Chiavone-Filho.

References

[1] L. Avaullee, L. Trassy, E. Neau, J.N. Jaubert, Fluid Phase Equilib. 141 (1997) 87–104.
[2] B. Lagourette, J.L. Daridon, J. Chem. Therm. 31 (1999) 987–1000.
[3] J.M. Smith, H.C. Van Ness, M.M. Abott, Introdução a Termodinâmica da Engenharia Química, 5th ed., LTC Publisher, Rio de Janeiro, 2000.
[4] K.S. Pitzer, S.M. Sterner, J. Chem. Phys. 101 (1994) 3111–3116.
[5] S.L. Randzio, U.K. Deiters, Phys. Chem. Chem. Phys. 99 (1995) 1179–1186.
[6] J. Gregorowicz, J.P. O’Connell, C.J. Peters, Fluid Phase Equilib. 116 (1996) 94–101.
[7] J.C. Hemptinne, P. Ungerer, Fluid Phase Equilib. 106 (1995) 81–109.
[8] D.Y. Peng, D.B. Robinson, Ind. Eng. Chem. Fundam. 15 (1976) 59–64.
[9] A. Péneloux, E. Rauzy, R. Frèze, Fluid Phase Equilib. 8 (1972) 7–23.
[10] E. Behar, R. Simonet, E. Rauzy, Fluid Phase Equilib. 21 (1985) 237–255.
[11] C.H. Chien, R.A. Greenkorn, K.C. Chao, AIChE J. 29 (1983) 560–571.
[12] B.I. Lee, M.G. Kesler, AIChE J. 25 (1975) 510–527.
[13] H.B. Sant’Ana, P. Ungerer, J.C. Hemptinne, Fluid Phase Equilib. 154 (1999) 193–204.
[14] P. Ungerer, C. Batut, Rev. L’Inst. Français Pétrole 52 (1997) 609–623.
[15] K. Nasrifar, S. Ayatollahi, M. Moshfeghian, Fluid Phase Equilib. 168 (2000) 149–163.
[16] L.C. Yen, S.S. Woods, AIChE J. 12 (1966) 95–99.
[17] P.L. Chueh, J.M. Prausnitz, AIChE J. 15 (1969) 471–472.
[18] S.W. Brelvi, J.P. O’Connell, AIChE J. 21 (1975) 171–173.
[19] G.H. Thomson, K.R. Brobst, R.W. Hankinson, AIChE J. 28 (1982) 671–676.
[20] H.Y. Lee, G. Liu, Fluid Phase Equilib. 108 (1995) 15–25.
[21] M. Aalto, K.I. Keskinen, J. Aittamaa, S. Liukkonen, Fluid Phase Equilib. 114 (1996) 1–19.
[22] H. Eslami, R. Azin, Fluid Phase Equilib. 209 (2003) 245–254.
[23] G. Parsafar, E.A. Mason, J. Phys. Chem. 97 (1993) 9048–9053.
[24] J.A. Amorim, O. Chiavone Filho, L.L. Marcio, K. Paredes, Rajagopal, J. Chem. Eng. Data 52 (2007) 613–618.
[25] F. Audonnet, A.A. Pádua, Fluid Phase Equilib. 216 (2004) 235–244.
[26] Y. Tanaka, H. Hosokawa, H. Kubota, T. Makita, Int. J. Thermophys. 12 (1991) 245–264.
[27] O. Redlich, A.T. Kister, C.E. Turnquist, Chem. Progr. Symp. Ser. 2 (48) (1952) 49–61.
[28] P.G. Tait, Physical and Chemistry of the Voyage of H.M.S. Challenger II. Part IV. S.P. LXI, H.M.S.O, London, 1888.
[29] J.O. Valderrama, L.A. Cisternas, Fluid Phase Equilib. 29 (1986) 431–438.
[30] R.C. Reid, J.M. Prausnitz, B.E. Poling, The Properties of Gases and Liquids, McGraw-Hill, New York, 1987.
[31] J.A. Nelder, R. Mead, Comput. J. 7 (1965) 308–313.